Seismic azimuthal anisotropy analysis for estimating reservoir properties at Stybarrow Field, NW Shelf, Australia

Lisa Jade Gavin, David Lumley and Jeffrey Shragge
Centre for Petroleum Geoscience and CO2 Sequestration, University of Western Australia, M004, 35 Stirling Hwy, Crawley WA 6009
gavinl01@student.uwa.edu.au, david.lumley@uwa.edu.au, jeffrey.shragge@uwa.edu.au

SUMMARY

Reservoir rocks are often subjected to anomalous vertical and/or horizontal stress conditions and may also contain complex physical attributes such as fracture sets. These rock properties are not easy to detect and map directly away from the borehole, but are sometimes indirectly evident in seismic data as azimuthal anisotropy. Thus, an analysis of anisotropic rock physics seismic attributes can be important for estimation of stress orientations and magnitudes, useful for reservoir evaluation, reducing drilling risks, and enhancing reservoir injection and production methods.

The Stybarrow field, located offshore NW Australia, is an example where seismic data exhibit strong azimuthal anisotropy, likely due to the effects of large horizontal tectonic stresses applied to the Carnarvon sedimentary basin. We find evidence for azimuthal anisotropy in AVO reflection amplitude difference maps and cross plots from two repeated 3D seismic surveys acquired at different azimuths, as well as in dipole shear logs and borehole breakout data. We model azimuthal AVO responses using Ruger's horizontal transverse isotropy (HTI) AVO equation, using the anisotropy parameters derived from dipole shear logs, and compare the results with AVO gathers from the two 3D seismic surveys with different acquisition azimuths. We use a least squares method to find the coordinate rotation and scaling factor that optimally matches the real seismic data to the modelled data predicted by Rüger's theory.

Key words: anisotropy, azimuth, stress, reservoir, reflection.

INTRODUCTION

Reservoir rocks may be subject to anomalous vertical or horizontal stress conditions and often contain complex stress-related features like fracture sets. Though these properties are not easy to detect and map directly away from the borehole, they are sometimes observable as seismic azimuthal anisotropy (AA). Stress orientation and magnitude are of critical importance for reservoir evaluation; proper estimation can greatly reduce drilling risks and enhance reservoir injection and production methods.

At a given point, variations in principle stress components can cause azimuthally variable velocities and reflection coefficients in seismic data. When a rock is under compressive stress compliant grain contacts will stiffen, increasing its elastic moduli (Mavko et al, 2003). This in turn increases wave velocity, because the (isotropic) P-wave velocity is proportional to both the bulk and shear modulus, and the S-wave depends on the shear modulus. Accordingly, horizontally dominated stress variations can lead to azimuthal dependent velocity profiles. Where these occur in a geologic layer above or below an interface, azimuthal variations in impedance contrast and reflection coefficients will result. This factor makes conventional isotropic AVO analysis more complex, and is commonly overlooked in standard seismic interpretations (many seismic data acquisition geometries do not contain a wide sampling of source-receiver azimuths.)

To facilitate numerical modelling, we assume that the AA media can be represented by a transversely isotropic medium with horizontal symmetry axis (HTI). Rüger (1998) derived a theoretical approximation for modelling reflection coefficients in weak HTI media. The anisotropic parameters within Rüger's (1998) equation were originally defined in terms of fast and slow velocities by Thomsen (1986).

The Stybarrow field located offshore NW Australia, is one geologic location where geophysical data exhibit evidence for significant AA. Observations of local AA are found in dipole shear logs and other geophysical data, and approximately match regional observations (Hillis and Reynolds, 2000). One goal of our work is to estimate and quantify the AA parameters, so that information about stress orientations can be interpreted from azimuthal variations in the seismic reflection data. This analysis may be useful for other sites in the Carnarvon Basin, where azimuthal anisotropy introduces complexity to seismic acquisition and processing flow designs.

In this paper we use 3D seismic reflection data to look for additional evidence of AA at the Stybarrow field. We use two repeated narrow-azimuth 3D seismic surveys acquired at different principle directions to generate azimuthally variable AVO reflection amplitude difference maps and crossplots. We use least squares optimization to find the coordinate rotation and scaling factors to optimally match actual seismic reflection amplitudes to modelled data predicted by Rüger's (1998) equations.

STYBARROW FIELD

The Stybarrow field is located approximately 65 km offshore Exmouth on the Northwest Australian coast. The field lies near the southern most extent of the Exmouth sub-basin within the Carnarvon Basin. It exhibits strong azimuthal anisotropy, likely due to the effects of horizontal tectonic stress on the

Carnarvon Basin. In Figure 1 the maximum horizontal stress direction from breakout data is indicated in red for the Carnarvon Basin.

Two 3D seismic surveys have been acquired over the area. Figure 1 shows a 51° difference in acquisition azimuth, where the first acquisition sail direction in 1998 and 2001 was 89°/269° and subsequent survey direction in 2008 was 35°/215°.

An example of a seismic cross section from Stybarrow Field is shown in Figure 3. The position of the Macedon Sand (coloured blue) is shown relative to other prominent horizons within the Carnarvon Basin, including the Top Muderong Shale, the Top Barrows, and Intra-Pyrenees.

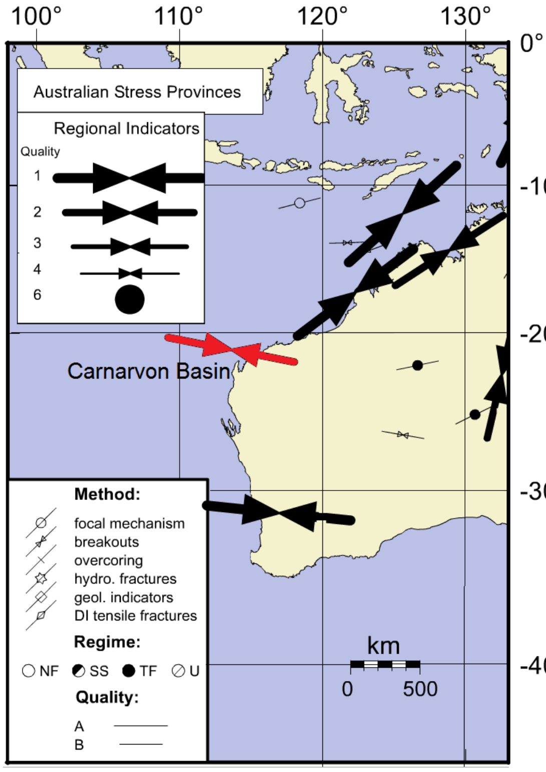

Figure 1. Maximum horizontal stress orientations from borehole breakout data in Western Australia. The red indicator shows the mean stress of the Carnarvon Basin near the location of the Stybarrow field. Adapted from Hillis and Reynolds (2000).

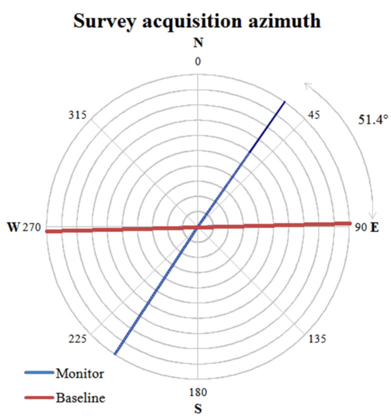

Figure 2. Seismic survey acquisition directions for the Stybarrow baseline and monitor surveys. Survey azimuthal difference is 51°.

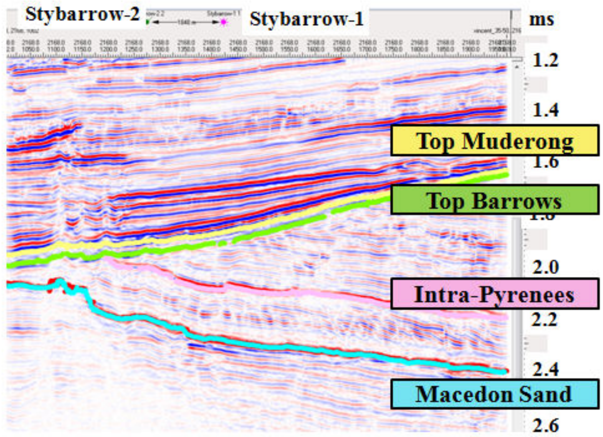

Figure 3. Seismic cross section showing the position of the Macedon Sand reservoir interface relative to the Top Muderong shale (no observed anisotropy), Top Barrows (start of shear wave anisotropy) and the Intra-Pyrenees event.

REFLECTION AMPLITUDES AND AVO

Azimuthal anisotropy is evident in amplitude difference maps between the two surveys acquired at different azimuths. The data was processed to preserve reflection amplitudes. The Top Macedon Sand interface was interpreted on both surveys and then amplitudes extracted. The anisotropy is evident in amplitude difference maps where the baseline amplitudes were subtracted from the monitor amplitudes (Figure 4). It is also demonstrated through amplitude cross plots of the two surveys, where the amplitude ratios deviate from unity (Figure 5).

The difference in reflection amplitudes suggests that the corresponding AVO curves will be proportionately different. To find the average AVO values from the seismic data the minimum amplitude at the Macedon Sand interface was extracted for incidence angle ranges 10-20°, 20-35° and 35°-50° for both surveys. Figure 4 shows the amplitude differences in what we term fault block B. We collected all amplitudes within the area indicated and found the mean value (example of amplitude statistics is shown in Figure 5).

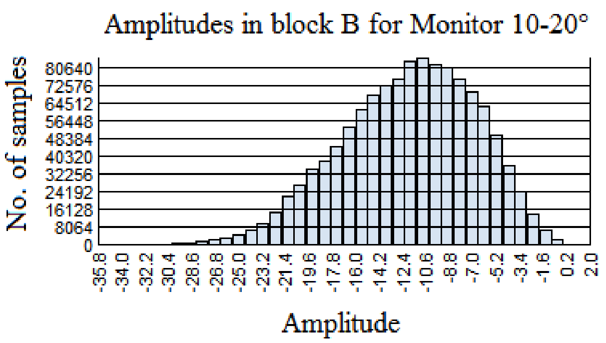

Figure 5. An example of amplitude statistics from fault block B for the incidence angle range 10-20° for the monitor survey.

MODELLING AZIMUTHAL AVO

Azimuthal AVO responses can be modelled using Ruger's (1998) horizontally transversely isotropic (HTI) azimuthally varying AVO equation:

$$R_p(i,\phi)=\frac{1}{2}\frac{\Delta Z}{\bar{Z}}+\frac{1}{2}\left\{\frac{\Delta\alpha}{\bar{\alpha}}-\left(\frac{2\bar{\beta}}{\bar{\alpha}}\right)^2\frac{\Delta G}{\bar{G}}+\left[\Delta\delta^{(v)}+2\left(\frac{2\bar{\beta}}{\bar{\alpha}}\right)^2\Delta\gamma\right]\cos^2\phi\right\}\sin^2 i$$

$$+\frac{1}{2}\left\{\frac{\Delta\alpha}{\bar{\alpha}}+\Delta\varepsilon^{(v)}\cos^4\phi+\Delta\delta^{(v)}\sin^2\phi\cos^2\phi\right\}\sin^2 i\tan^2 i \quad (1)$$

where i is the incident angle, □ the azimuthal angle from the symmetry axis plane, α the vertical P-wave velocity, β the vertical S-wave velocity, Z the vertical P-wave impedance $Z = \rho\alpha_{\|}$, the subscripts ‖ and ⊥ refer to the fast and slow P- and S-waves respectively, G the vertical shear modulus $G = \rho\beta_{\|}^2$. The average velocity $\bar{\alpha} = 1/2(\alpha_2 + \alpha_1)$ and the difference $\Delta\alpha = (\alpha_2 - \alpha_1)$, the subscripts 1 and 2 correspond to the first and second medium respectively. γ, ε and δ are the anisotropic Thomsen parameters (Thomsen, 1986, Contreras et al., 1999) which can be defined in terms of fast and slow velocities.

The Thomsen parameters can be related to the underlying stiffness matrix (here in the 6x6 Voigt notation) (Thomsen, 1988). The P-wave fractional difference in the [x1, x3] plane, ϵ. is given by:

$$\varepsilon^{(V)} = \frac{C_{11}-C_{33}}{2C_{33}} = \frac{\alpha_\perp^2\rho-\alpha_\|^2\rho}{2\alpha_\|^2\rho} \quad ; \quad (2)$$

the S-wave fractional difference in the [x1, x3] plane, γ, is:

$$\gamma^{(V)} = \frac{C_{66}-C_{44}}{2C_{44}} = \frac{\beta_\perp^2\rho-\beta_\|^2\rho}{2\beta_\|^2\rho} \; ; \quad (3)$$

A Thomsen-style parameter, responsible for near vertical P-wave velocity and that influences the velocity of the in-plane polarized S-wave, δ:

$$\delta^{(V)} \equiv \frac{(C_{13}-C_{55})^2-(C_{33}-C_{55})^2}{2C_{33}(C_{33}-C_{55})} = \frac{(C_{13}-\beta_\perp^2\rho)^2-(\alpha_\perp^2\rho-\beta_\perp^2\rho)^2}{2\alpha_\perp^2\rho(\alpha_\perp^2\rho-\beta_\perp^2\rho)} \quad (4)$$

which was approximated by Thomsen's (1988) formulation:

$$\delta \approx \varepsilon - \gamma\left(\frac{\beta_\|^2}{\alpha_\|^2}\right); \quad (5)$$

where the C_{ij} terms come from the elastic stiffness tensor and are written in Voigt notation. Some of these terms can be written in terms of fast and slow P- and S-wave velocities and density (Thomsen, 1986, Contreras et al., 1999) as shown in Equations 2, 3 and 5.

The fast and slow P- and S-wave velocity and density values at Stybarrow were estimated from averaged dipole shear log measurements from exploration wells.

ANISOTROPY ANALYSIS

Observed reflection amplitudes need to be multiplied by a scalar (calibrated) to be compared to theoretical reflection coefficients. The scaling factor and the theoretical azimuth of incidence for Stybarrow data were both unknown; to find them we used a least squares error approach.

The result of the scaling factor and theoretical azimuth estimates (monitor 102° and baseline 53°) in Figure 6 seem reasonable, especially considering that the seismic amplitudes derived from super gathers containing a range of azimuths and reflection angles. There is a 49° difference between the two theoretical azimuths which is only 2° off the actual difference between the two survey acquisition azimuths. The theoretical and observed amplitudes correlate within reasonable range.

The coordinate rotation that optimally matches the seismic data from that predicted from Rüger's (1998) theory is consistent with the interpretation done by BHP Billiton Petroleum to acquire the seismic along the slow HTI axis.

CONCLUSIONS

This paper demonstrates that HTI anisotropy is present in the Stybarrow field. It is evident in AVO reflection amplitude difference maps and cross plots from two repeated 3D surveys acquired at different azimuths, AVO gathers and dipole shear log data. We used a least squares method to estimate a coordinate rotation and scaling factor that optimally matches the actual seismic data to synthetic data predicted by Rüger's equation. The slow and fast velocity directions we estimate are consistent with the interpretation done by BHP.

ACKNOWLEDGMENTS

We would like to acknowledge Guy Duncan and Robin Hill at BHP Billiton Petroleum for allowing us to use the Stybarrow data, the ASEG Research Foundation for their grant to LG, and the sponsors of the UWA Reservoir Management (UWA:RM) industry research consortium. LG was also supported by a UWA Gledden Scholarship.

REFERENCES

Contreras, P., Grechka, V. & Tsvankin, I., 1999, Moveout inversion of P-wave data for horizontal transverse isotropy: Geophysics, 64, 1219-1229.

Hillis, R. R. & Reynolds, S. D., 2000, The Australian stress map: Journal of the Geological Society, 157, 915-921.

Mavko,G., Mukerji, T. & Dvorkin, J., 2003, Rock Physics Handbook – Tools for Seismic Analysis in Porous Media: Cambridge University Press.

Rüger, A., 1998, Variation of P-wave reflectivity with offset and azimuth in anisotropic media: Geophysics, 63, 935-947.

Thomsen, L., 1988, Reflection seismology over azimuthally anisotropic media: Geophysics, 53, 304-313.

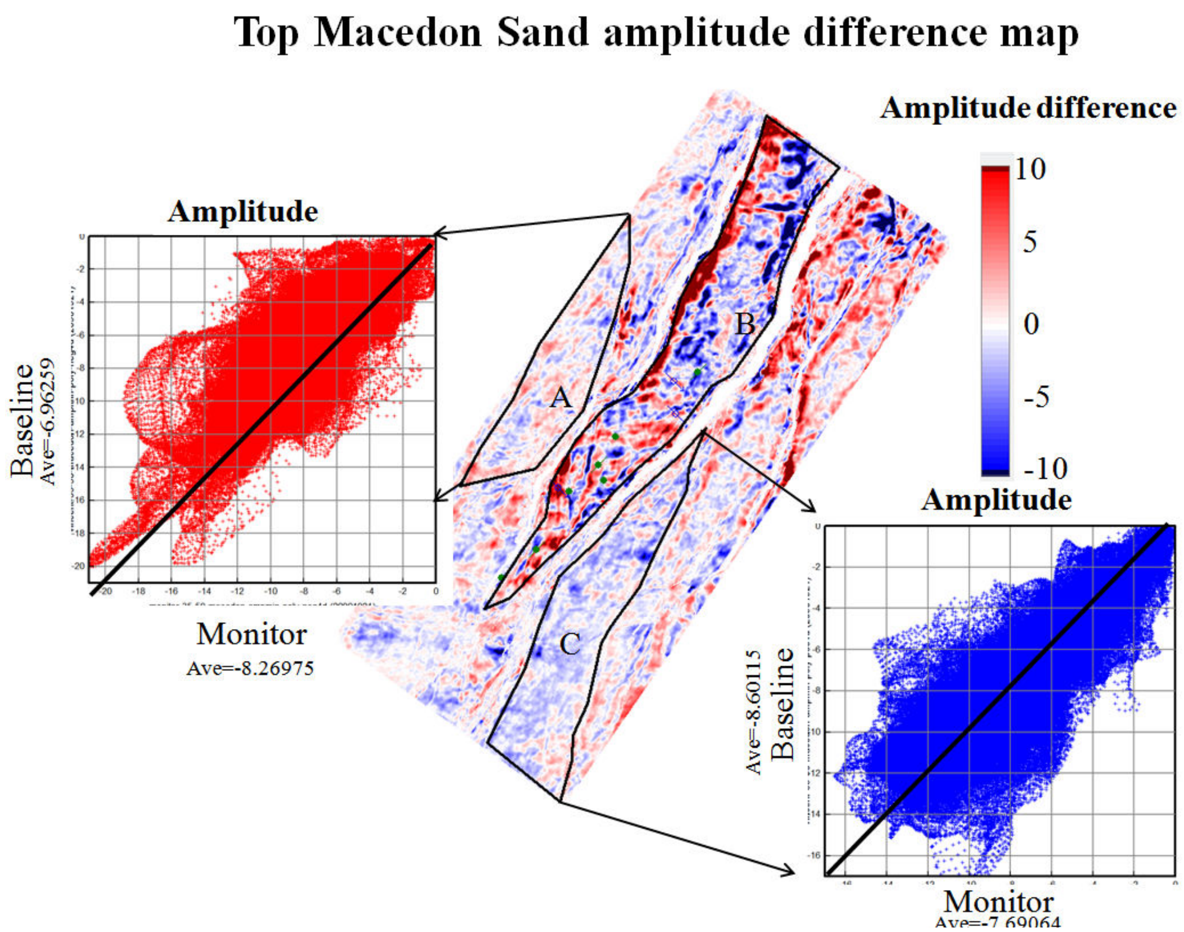

Figure 4. **Amplitude *difference* map of the Macedon Sand interval, where the Baseline survey result is subtracted from the Monitor survey. The crossplots are from the fault blocks in section A and C, and show that amplitudes for the two surveys are different consistent with the different azimuth of the survey direction.**

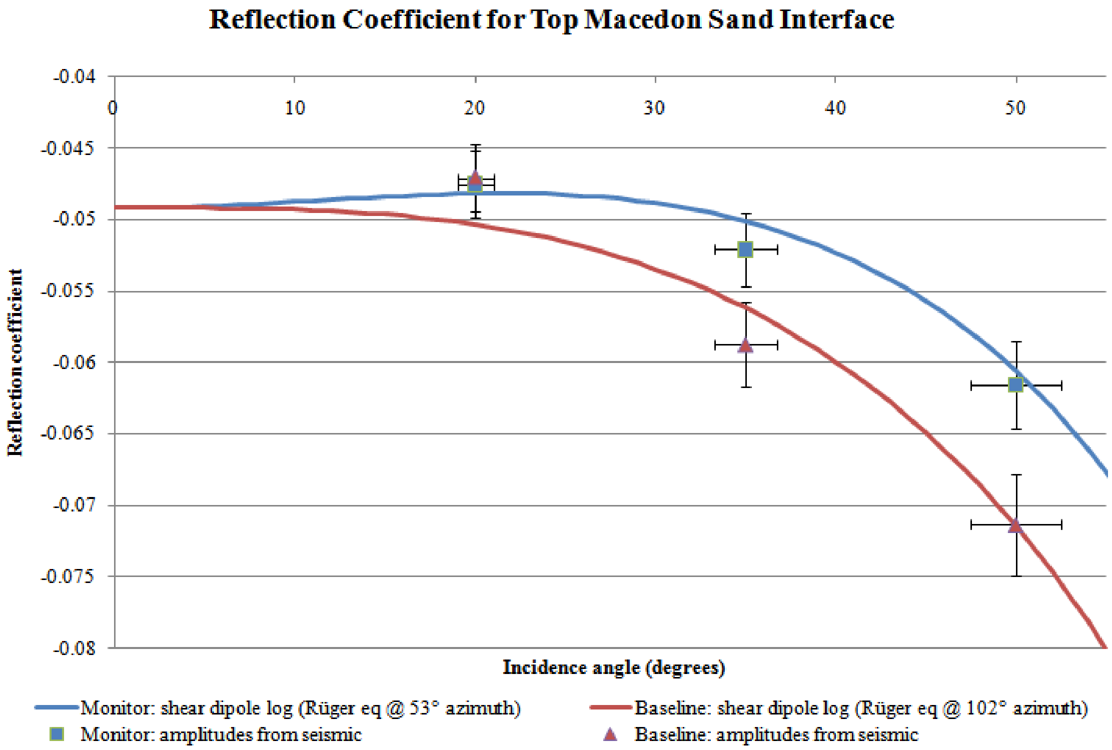

Figure 6. **Comparison of reflection coefficients extracted from Stybarrow seismic data to HTI modelling results using Rüger's equation and Stybarrow geophysical log data.**